

Inhibitors of Polo-like kinase reveal roles in spindle-pole maintenance

Campbell McInnes^{1,5,6}, Aavek Mazumdar^{2,6}, Mokdad Mezna^{1,5}, Christopher Meades¹, Carol Midgley³, Fred Scaerou³, Lee Carpenter², Mairi Mackenzie¹, Paul Taylor⁴, Malcolm Walkinshaw⁴, Peter M Fischer^{1,5} & David Glover^{2,3}

Polo-like kinases (Plks) have several functions in mitotic progression and are upregulated in many tumor types. Small-molecule Plk inhibitors would be valuable as tools for studying Plk biology and for developing antitumor agents. Guided by homology modeling of the Plk1 kinase domain, we have discovered a chemical series that shows potent and selective Plk1 inhibition. The effects of one such optimized benzthiazole *N*-oxide, cyclapolin 1 (1), on purified centrosomes indicate that Plks are required to generate MPM2 epitopes, recruit γ -tubulin and enable nucleation of microtubules. The compound can also promote loss of centrosome integrity and microtubule nucleating ability apparently through increased accessibility of protein phosphatases. We show that treatment of living S2 cells with cyclapolin 1 leads to collapsed spindles, in contrast to the metaphase-arrested bipolar spindles observed after RNAi. This different response to protein depletion and protein inhibition may have significance in the development of antitumor agents.

The Polo-like kinases are named after the *polo* mutant of *Drosophila melanogaster* and belong to a conserved subfamily of serine/threonine protein kinases that have conserved functions in mitotic progression^{1–3}. Whereas both budding yeast and fission yeast have only one Plk, three closely related kinases (Plk1, Plk2 and Plk3) and one more distantly related enzyme (Plk4, or Sak) have been identified in mammals⁴. Plks have an N-terminal catalytic domain and a C-terminal domain that contain two conserved regions (in Plk1, Plk2 and Plk3)⁵, or one in the case of Plk4 (ref. 6), termed the Polo boxes. The Polo boxes are implicated in cellular localization and compartmentalization of Plks, which is most likely achieved by mediating interactions with substrates (for example, the phosphatase Cdc25C)^{5,7}. The ability of the Polo box to bind a specific phosphopeptide has led to a model whereby a substrate is first phosphorylated by a priming kinase to facilitate subsequent phosphorylation by Plk. At the same time, the Polo-box domain has been proposed to act as an autoregulatory domain, a notion consistent with the finding that expression of C-terminally truncated Plk1 results in an increase in kinase activity⁸.

Plk1 functions at several mitotic stages. It regulates mitotic entry through the phosphorylation and activation of Cdc25 (ref. 9), thereby participating in the positive activation loop for the cyclin-dependent kinase 1 (Cdk1)–cyclin B complex. In parallel, the phosphorylation of Wee1 by Plk1, which is primed by Cdk1, promotes the destruction of this inhibitor of mitotic entry¹⁰. Plk1 also regulates these processes through the checkpoint kinases in response to DNA damage¹¹. Mitotic entry is associated with the maturation of the centrosomes, for which

Polo kinase is required to recruit the γ -tubulin ring complex (γ -TuRC) and activate molecules such as the abnormal spindle protein (Asp) to promote microtubule nucleation¹². Plks promote anaphase-promoting complex/cyclosome (APC/C) activation by phosphorylating the APC/C inhibitor Emi1 (refs. 13,14) or the related Erp1 (refs. 15–17), which targets these molecules for proteolysis. The separation of chromatids first requires Plk1 to phosphorylate sister chromatid cohesin 1 (SCC1) and its ortholog SA2, which then mediate dissociation of the cohesin complex from chromosome arms in prophase and prometaphase¹⁸. Shugoshin (also called MeiS332), which protects centromeric cohesin, is removed from centromeres after Polo phosphorylation¹⁹, and the Polo-mediated phosphorylation of SCC1 enhances its susceptibility to proteolytic cleavage²⁰. These kinetochore functions seem interrelated to the spindle-integrity checkpoint given that the phosphopeptide 3F3/2, which senses the lack of tension at the kinetochore, is generated through Plk1 activity^{21,22}. Finally, the Plks are also required for cytokinesis through interaction with and phosphorylation of the MKLP1 family of motor proteins^{23–26}. Plk1 itself is a target of the APC, and its degradation contributes to exit from mitosis²⁷.

Overexpression of Plk1 is frequently observed in human tumors and can have prognostic value. Moreover, downregulation of Plk1 by antisense oligonucleotides and small interfering RNA (siRNA) is highly effective in inhibiting cancer-cell proliferation both *in vitro* and *in vivo*^{28,29}.

The natural product scytonemin (2) was one of the first Plk1 inhibitors to be characterized, but it is a weak and nonselective

¹Cyclacel Ltd., James Lindsay Place, Dundee DD1 5JJ, UK. ²Cancer Research UK Cell Cycle Genetics Research Group, University of Cambridge, Department of Genetics, Downing Street, Cambridge CB2 3EH, UK. ³Cyclacel Ltd., Polgen Laboratories, Babraham Science Park, Cambridge CB2 4AT, UK. ⁴Department of Structural Biochemistry, University of Edinburgh, Edinburgh EH9 3JR, UK. Correspondence should be addressed to D.G. (dmg25@hermes.cam.ac.uk). ⁵Present addresses: College of Pharmacy, University of South Carolina, Columbia, SC 29208 (C.Mc.), Beatson Institute, Glasgow G61 1BD, UK (M.M.) and School of Pharmacy, University of Nottingham, Nottingham NG7 2RD, UK (P.M.F.). ⁶These authors contributed equally to this work.

Received 9 February; accepted 24 August; published online 8 October 2006; doi:10.1038/nchembio825

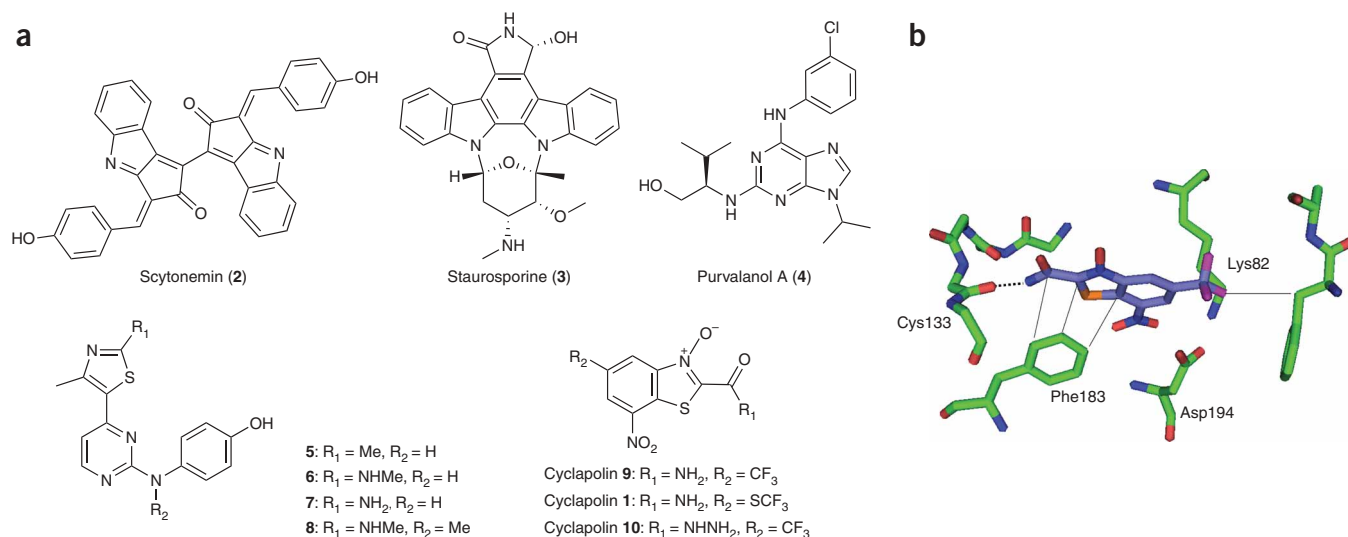


Figure 1 Chemical structures of Plk1 inhibitors. **(a)** Compounds identified through *in vitro* screening of known kinase inhibitors (**2**, **3**, **4**, **5**, **6** and **7**) and used for validation of the homology structure generated for the kinase domain of Plk1. **9** was identified through *in silico* screening and further analogs in this series (**1** and **10**) were generated. **(b)** Molecular docking of **9** with the active site led to the proposed binding mode of benzthiazole *N*-oxide Plk1 inhibitors with the ATP binding site of Plk1.

molecule. Although more specific compounds have been described³, there has been a surprising lack of progress, and hence there is considerable scope for further development of potent and selective inhibitors. Here we describe a structure-guided design approach to the discovery and development of benzthiazole *N*-oxide Plk1 inhibitors and show that treatment of both *D. melanogaster* and human cells with compounds from this series result in the formation of abnormal spindles that are characteristic of Polo kinase inhibition. Moreover, the effects of these compounds on the ability of partially purified centrosomes to nucleate asters of microtubules *in vitro* indicate roles for Polo kinase in the maturation of the centrosomes and in the maintenance of their microtubule nucleating properties.

RESULTS

Construction of a Plk1 kinase-domain homology structure

To pursue a structure-guided approach to the discovery of Plk1 inhibitors, we generated a homology model of the kinase domain of Plk1. Though crystal structures have recently been determined for the Polo-box region of Plk1, there is currently no experimental structural information available for the kinase domain. We used the staurosporine (**3**)-bound conformation of protein kinase A (PKA) to generate a model structure and several known Plk1 inhibitors to validate this hypothetical structure before using it in high-throughput ligand-docking calculations. Previously we demonstrated that purvalanol A (**4**) (**Fig. 1a**) and a set of thiazoloanilopyrimidine compounds are micromolar Plk1 inhibitors³. In the first instance, we positioned **4** in the Plk1 active site using a flexible docking routine, and after energetic ranking of poses, a conformation was found that had intermolecular contacts appropriate for kinase inhibition and similar to the binding mode with Cdk2. As a control, we docked **4** (which does not inhibit the kinase activity of PKA) with the structural template used in the model building (1STC). In agreement with the lack of activity of **4**, none of the predicted binding modes of this inhibitor formed interactions that are consistent with kinase inhibition. Additional calculations using a series of Plk1 inhibitors with an existing structure-activity relationship (**5**, **6**, **7** and **8**; **Fig. 1**) confirmed that the homology structure can be

used to facilitate structure-guided design. The two structures containing an aliphatic substituent at this position, **5** (half-maximal inhibitory concentration (IC₅₀) = 5 μM) and **6** (IC₅₀ = 10 μM), are more potent than the compound containing a primary amine substitution, **7** (IC₅₀ = 25 μM). Examination of the interactions of these docked structures suggests a Cdk2-like binding mode and a correlation of the structure-activity relationship (SAR) of the two-position substituent with the inhibition constants. The essential role of the *p*-hydroxyaniline group of this series is suggested by the hydrogen bonding contacts with Arg135, and the increased potency of the aliphatic-substituted inhibitors on the thiazole can be rationalized by interactions of this group with Phe64, which could not be present in the 2-aminothiazole compound. To confirm that these compounds bind as proposed (and that their binding is similar to the conformation observed with Cdk2), we generated **8** with the aniline *N*-methylated to abrogate hydrogen bonding to the hinge region. We found this compound to be inactive in the Plk1 kinase assay. As inhibitor docking with the homology structure was successful, we considered the model to be sufficiently validated for further structure-guided design of Plk1 inhibitors.

Discovery of potent and selective inhibitors of Plk1 using LIDAEUS

Using the complex of **5** with the Plk1 kinase domain model, we used LIDAEUS³⁰, a tool for rapid flexible docking of ligands into protein binding sites, to dock a library of 200,000 commercially available small molecules. Using this process, we assayed 350 *in silico* ranked compounds for their ability to inhibit Plk1 phosphorylation of Cdc25C by baculovirus-expressed Plk1 kinase. This strategy allowed us to identify Plk1 inhibitors with potencies ranging from 0.5 to 20 μM. The most potent inhibitor identified from virtual screening, which we term cyclapolin 9 (**9**), has a benzthiazole *N*-oxide core structure (**Fig. 1a**).

To further explore the SAR of this series, we developed a synthetic route for the benzthiazole *N*-oxide and generated analogs related to **9** (**Fig. 1a**). A description of the SAR in a series of compounds based on this benzthiazole *N*-oxide core will be presented elsewhere. Here we will focus on the properties of cyclapolin 1, in which the CF₃ group

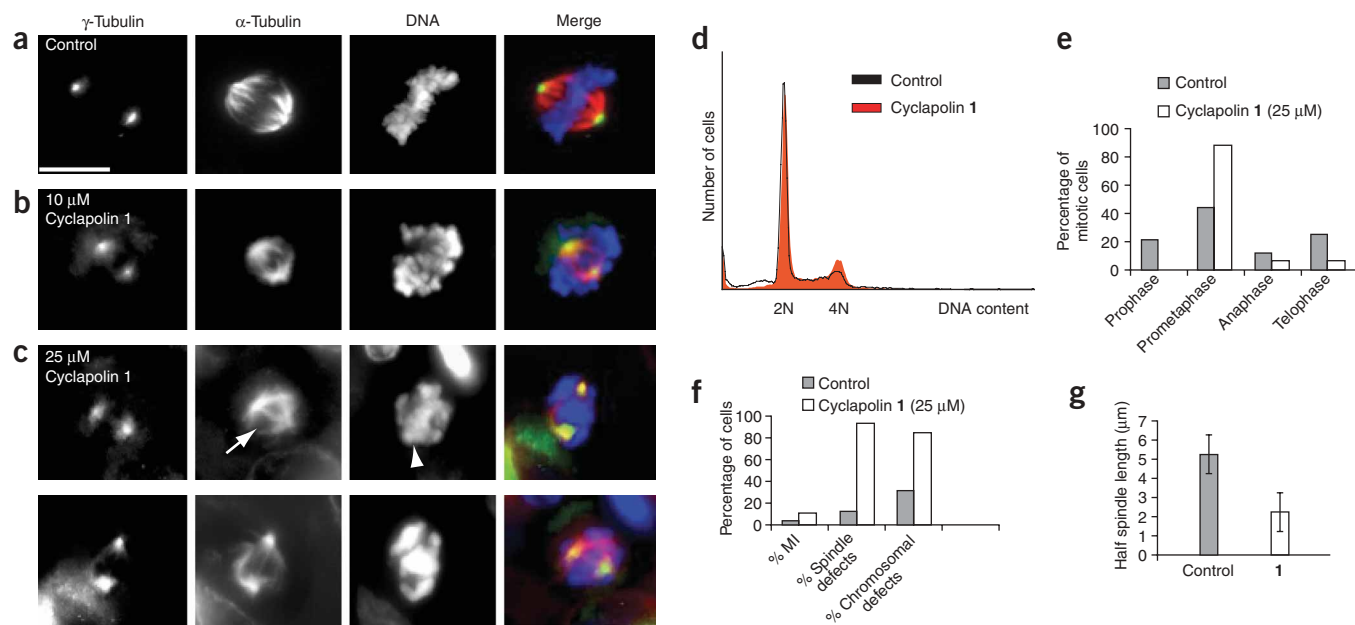


Figure 2 Mitotic abnormalities induced by cyclapolin 1 in HeLa cells. (**a–c**) HeLa cells were treated with 0.1% DMSO (control) (**a**) or **1** (10 μM and 25 μM) (**b,c**) for 24 h before fixing and staining to reveal α-tubulin (red), γ-tubulin (green) and DNA (blue). (**d**) Flow cytometry showed an increase in 4N cells (G2 and M) after **1** treatment and an increase in sub-G1 cells, which is indicative of apoptosis. (**e**) Proportions of cells at different stages of mitosis. (**f**) Proportions of cells with the indicated mitotic defects are shown in the histograms. Scale bar represents 10 μm. MI, mitotic index. (**g**) Spindle lengths were measured as pole-to-pole distances using Metamorph software (Universal Imaging).

was replaced with a trifluoromethylthioether. This substitution resulted in a substantial increase in potency, from an IC_{50} of 500 nM to an IC_{50} of approximately 20 nM, which suggests more complementary interactions of the CF_3 group in the ATP binding site. Further synthetic modification of the substituents on the thiazole ring revealed that replacing the amide with a hydrazide derivative in cyclapolin **10** results in an inactive compound.

To assess the binding of the benzthiazole *N*-oxide lead compounds in the Plk1 ATP cleft, we carried out rigorous molecular docking experiments using the Plk1 model structure. We evaluated numerous docking solutions in terms of interaction energy and docking score, and with respect to known kinase inhibitory interactions, and we observed a binding mode that fulfilled each of these criteria (**Fig. 1b**). There was a good correlation between the nonbonded docking score and the potency of additional analogs from this series (data not shown). The CF_3S analog, **1**, deviated most in its docking score from other compounds in the series, which suggests that additional factors may contribute to binding. Our preliminary studies suggest that binding of **1** is noncompetitive with respect to ATP (**Supplementary Methods** and **Supplementary Fig. 1** online). We are currently investigating whether a covalent interaction of **1** with a residue in the ATP binding cleft explains the independence of binding with respect to ATP concentration, and also the observed potency increase.

We tested the benzthiazole series of compounds on a panel of 18 enzymes held in house by Cyclacel Ltd. (**Supplementary Table 1** online). None of these were inhibited by the *in silico*-identified lead cyclapolin **9**, or the more potent **1**. To further probe the selectivity of this compound, we examined a further 20 kinases available from an outsourced screen for inhibition in the presence of 100 μM of **9** (**Supplementary Methods** and **Supplementary Table 1**). Notably, none of the enzymes in this additional panel showed a significant level of inhibition, with the exception of C-terminal Src kinase, whose

activity was slightly blocked by the action of this compound (<50% inhibition at 100 μM of compound). In addition to discovering these potent and selective inhibitors, we performed studies to determine the cellular consequences of Plk1 inhibition. In the first instance, we determined the cytotoxic effect of the compounds in an assay for cytotoxicity on cultured human cells (**Supplementary Methods** and **Supplementary Table 2** online). The cell lines tested varied in sensitivity to the cyclapolins, with HeLa and HT-29 cells being the most sensitive, and the inactive Plk1 inhibitor **10** did not show significant cell growth inhibition. We therefore chose to examine the effects of **1** on mitotic progression in HeLa cells (**Supplementary Table 3** online).

Treatment of HeLa cells with cyclapolin 1 leads to an accumulation of mitotic cells with spindle abnormalities

Many phenotypes have been reported after the loss of Plk1 activity in human cells as a result of microinjection of antibodies to Plk1 or RNA interference (RNAi). Depending on the cell type, the effects range from arrest in G2 to a variety of spindle defects^{31,32}. Consistent with previous reports, we found that downregulation of Plk1 in HeLa cells by siRNA results in an elevation of the proportion of 4N cells observed by flow cytometry and of sub-2N cells, which is indicative of cell death. This was accompanied by a two- to three-fold increase in mitotic index, which reflects an accumulation of monopolar mitotic cells and cells with shortened spindles that may have unfocused poles (**Supplementary Fig. 1**). We also found an increase in 4N cells after treatment of HeLa cells with **1** for 24 h (**Fig. 2**), although this increase was less pronounced than that described above (**Fig. 2d**), that was associated with a similar two- to three-fold increase in mitotic index, most of the mitotic cells being in prometaphase (**Fig. 2e**). Immunostaining fixed preparations of such cells revealed that most spindles were shortened to less than 50% of the length of control-cell spindles

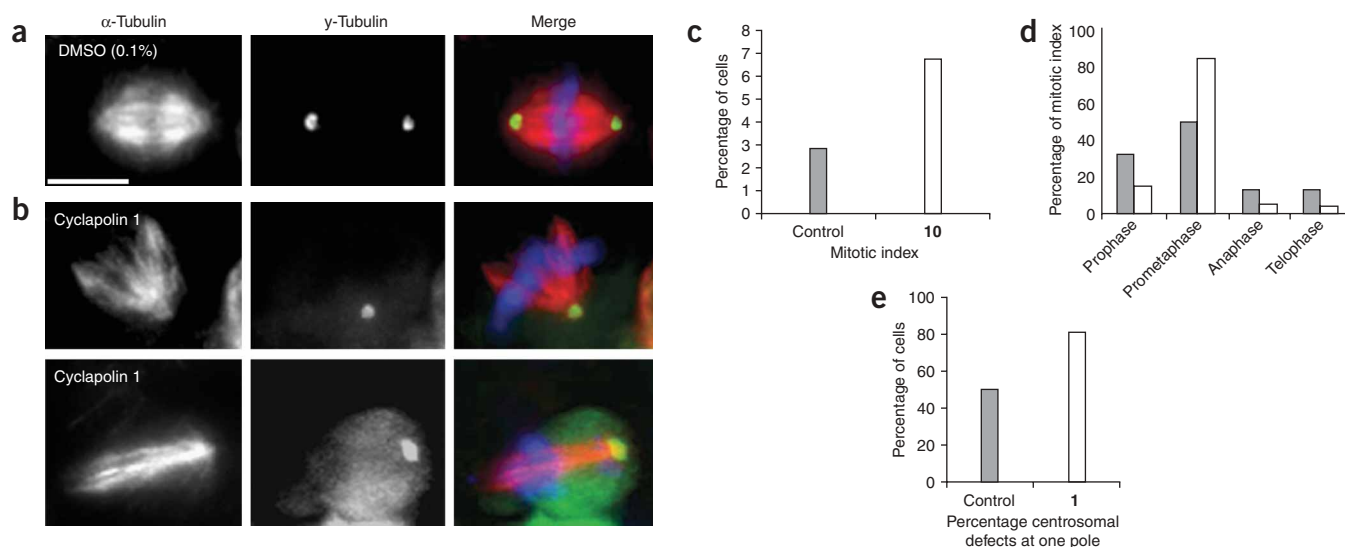


Figure 3 Cyclapolin 1 induces monopolar spindles in S2 cells. **(a,b)** *D. melanogaster* S2 cells after treatment with 0.1% DMSO **(a)** or **1** (10 μ M) **(b)** for 24 h and fixed for immunostaining to show α -tubulin (red), γ -tubulin (green) and DNA (blue). Scale bar represents 10 μ m. **(c)** Proportion of mitotic cells and mitotic defects. **(d)** Proportion of cells at different mitotic stages. **(e)** Percentage of centrosomal defects at one pole represents cells lacking a centrosome at one pole.

(Fig. 2b,c,g) and typically had a lower density of microtubules, whether cells were treated with 10 μ M or 25 μ M of **1**. At the higher concentration of the compound, the density of kinetochore microtubules seemed to be particularly affected, and it was more difficult to detect individual chromatids. Thus, treatment of asynchronous HeLa cells with the Plk inhibitor **1** leads to a loss of robust spindles that could be a result either of a failure of the spindle to fully elongate or of its partial collapse. However, this loss was not as extreme as the increase in monopolar spindles and spindles with unfocused poles observed after downregulation of Plk1 protein concentrations by RNAi (Supplementary Fig. 1).

Cyclapolin 1 treatment of *D. melanogaster* S2 cells results in both spindle collapse and loss of spindle-pole organization

Previous studies of *polo* in *D. melanogaster* suggests that different phenotypes arise depending on whether a mutation inactivates the kinase or reduces the concentration of protein. Thus we wondered whether treatment of *D. melanogaster* S2 cells with **1** results in a phenotype similar to that resulting from the depletion of Polo protein caused by RNAi or observed in the P-element mutants, *polo*⁹ and *polo*¹⁰ (refs. 33,34), or whether such treatment results in reduced catalytic activity of Polo, as seen in the original *polo*¹ allele^{1,2}. We found that **1** resulted in a two- to three-fold increase in mitotic index as a consequence of an increased proportion of prometaphase cells (Fig. 3). Approximately 80% of the mitotic cells had bipolar spindles that appeared to have either a single centrosome or both centrosomes at one pole (Fig. 3b,e). The other pole was typically broad and unfocused, but to varying extents. Thus, the above defects resemble those originally seen in the *polo*¹ mutant cells more than those seen in either the *polo*⁹ or *polo*¹⁰ mutants, or after Polo protein depletion by RNAi. There was no effect on the mitotic phosphorylation of histone H3 on Ser10, which indicates that the compound has no effect on Aurora B kinase (Supplementary Fig. 2 online). The effects of **1** treatment of HeLa and S2 cells were not reversible.

Time-lapse studies of S2 cells expressing green fluorescent protein (GFP)-tubulin revealed the way in which these abnormal spindles arise after **1** treatment. Whereas in control cells bipolar spindles elongated

in anaphase B and then formed the central spindle structure before undertaking cytokinesis (Fig. 4a), the spindles of cells treated with **1** remained short or collapsed and then recovered in one of two ways. The first is exemplified by the cell shown in the time-lapse series in which cells were treated with the compound once they had already entered mitosis (Fig. 4b). The spindle of this cell originally had highly focused poles, but one of these became progressively broader (from the 25-min time point), eventually extending to the opposite cortex of the cell (Fig. 4b). Thus one consequence of Polo kinase inhibition is the loss of focused microtubules at one spindle pole. The final outcome of such time-lapse series was very similar to that of the fixed preparation illustrated in Figure 4b, in which microtubules are focused on the centrosomal material at one pole, whereas the other pole is unfocused.

The second response (Fig. 4c) resulted in spindle collapse on **1** treatment, the two spindle poles becoming progressively closer such that a monopolar structure was formed (13-min time point). However, bipolarity was then reestablished (17 min onwards). Although chromosomes are not labeled, their positions can be discerned as a 'shadow' in the GFP fluorescence from which microtubules appear to be nucleated to extend and form a less focused pole (Fig. 4c). Thus a second consequence of Polo kinase inhibition is that kinetochore microtubules shorten, thereby resulting in a monopolar structure. This is a transient state from which bipolarity can be established, apparently as a result of microtubule nucleation from chromosomes, in which case the newly generated pole is unfocused. The subsequent lengthening of the spindle, which is suggestive of anaphase, has also been described in S2 cells when spindles collapse and then recover their bipolarity after depletion of microtubule-stabilizing protein Klp10A. The final outcome of time-lapse series of this type was similar to that of the fixed preparations in Figure 3b, in which an elongated spindle spanned the cell, with one pole clearly having two aggregated centrosomes.

Cyclapolin 1 inhibits the recruitment, activation and maintenance of the microtubule nucleating activity of centrosomes

The above observations suggest that inhibition of Polo kinase by **1** affects several aspects of centrosome behavior. To demonstrate that

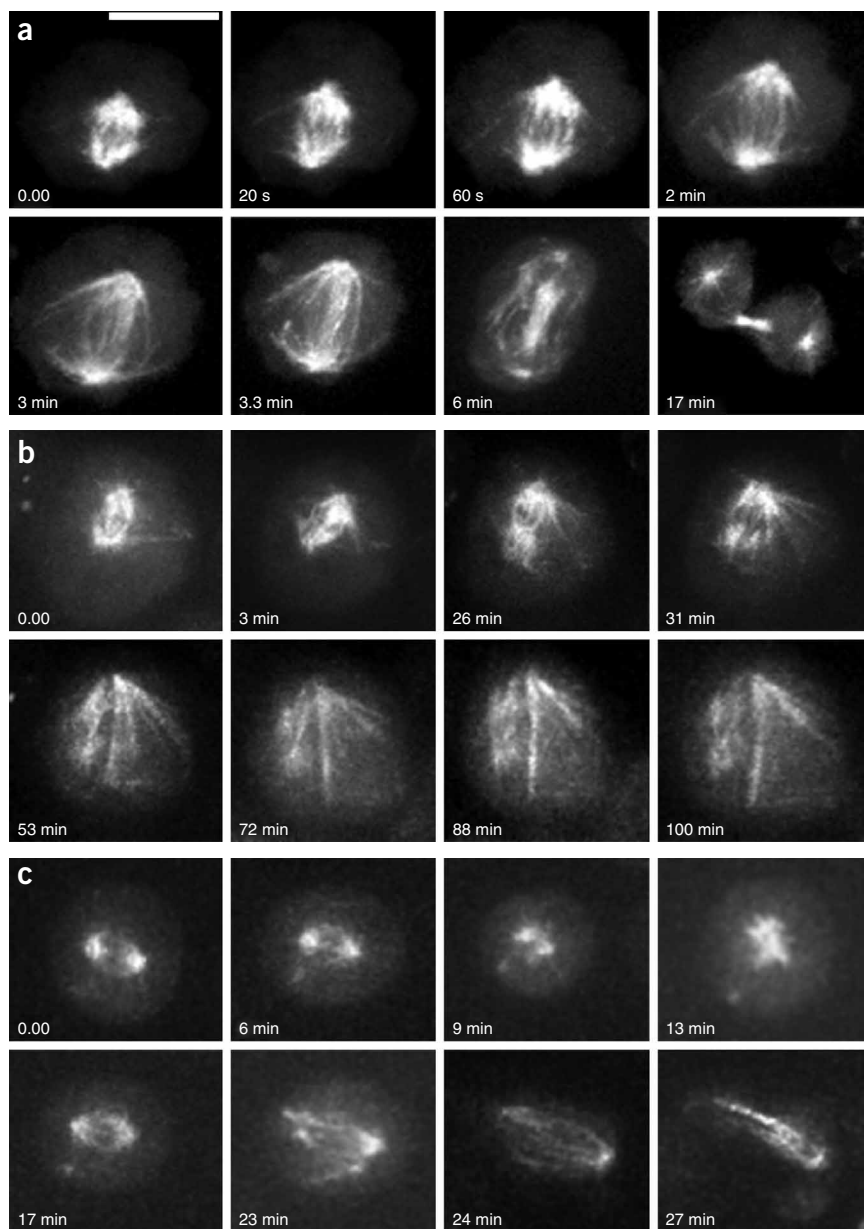


Figure 4 Time-lapse series of control and **1**-treated S2 cells. (a) Control cells. (b,c) **1**-treated cells. Selected frames are presented at the indicated time points from time-lapse sequences of S2 cells expressing GFP-tubulin. 25 μM **1** was added at time 0, when cells had already entered mitosis. Scale bar represents 10 μm . Movies showing the entire time series for each of these examples are presented in **Supplementary Methods**.

this effect may be mediated directly by inhibition of biological functions attributable to Plks, we used an *in vitro* system for the nucleation of microtubules by a preparation of centrosomes purified from *D. melanogaster* embryos. We found that *D. melanogaster* Polo kinase activity is inhibited by **1** at concentrations comparable to those required to inhibit human PLK1 (**Fig. 5a**). We then monitored the ability of a preparation of *D. melanogaster* centrosomes to nucleate asters of rhodamine-labeled tubulin in the presence of benzothiazole compounds. We began to see a reduction in the density of microtubules nucleated at 10 nM **1**, and at 20 nM, no microtubules were nucleated at all. In contrast, 20 nM **10** had no effect on Polo kinase activity or on the *in vitro* nucleation of microtubules by centrosomes

(**Fig. 5a,b**). We found that the ability of centrosomes to nucleate microtubules after **1** treatment can be restored by addition of a high-speed cytoplasmic supernatant, but not by such an extract from which Polo kinase has been immunodepleted (**Fig. 5c,d**). Thus we conclude that interaction of centrosomal Polo kinase with **1** inhibits the ability of centrosomes to nucleate microtubules in a manner that can be rescued by exogenously supplied Polo kinase.

We have previously shown that Polo activity is required to generate MPM2 epitopes on Asp, the product of the *abnormal spindle* gene that is required, together with the γ -TuRC, for microtubule nucleation³⁵. We found that **1** treatment results in the loss of γ -tubulin and the MPM2 epitope from centrosomes *in vitro* (**Fig. 5**). This correlated with a reduction in the number of centrosomes capable of nucleating astral microtubules (**Fig. 5h**) and was found to occur at concentrations of **1** corresponding to those required for inhibition of Polo kinase activity (**Supplementary Fig. 3** online). The molecular mass of one particular centrosomal protein that loses its MPM2 epitope on **1** treatment is consistent with it being Asp (**Fig. 5g**). Thus the interaction of **1** with Polo kinase at concentrations that inhibit its kinase activity and that could possibly also induce change in enzyme conformation seems to allow access of protein phosphatases that dephosphorylate centrosome-associated MPM2 epitopes. This effect is associated with loss of the γ -TuRC (and therefore loss of the ability of centrosomes to nucleate microtubules). We consistently found that treatment of the centrosome preparation with λ -phosphatase can also mediate the loss of MPM2 epitopes and γ -tubulin in the absence of **1** treatment (**Supplementary Fig. 3**). Together these results suggest that either continued Polo kinase activity or maintenance of Polo in an active conformation is necessary to protect centrosomal proteins from protein phosphatase activity in order to maintain the organization and function of the mitotic centrosome. Whereas the above assay tests the effect of Polo inhibition on the

ability of intact centrosomes to nucleate microtubules, it is also possible to model the recruitment of microtubule-nucleating molecules to centrosomes in an alternative assay. This involves stripping centrosomes to their core components by treating them with 1 M KI to remove their ability to nucleate microtubules (**Fig. 6**). Addition of a high-speed supernatant of syncytial embryo cytoplasm then results in recruitment of the γ -TuRC and Asp protein (not shown) and restoration of the MPM2 epitope and the ability to nucleate microtubules (**Fig. 6b**). Treatment of the cytoplasmic extract with 20 nM **1** resulted in the loss of the MPM2 epitope from a large number of proteins in the total extract. However, it did not prevent the ability of exogenous rhodamine-labeled tubulin to participate in forming long

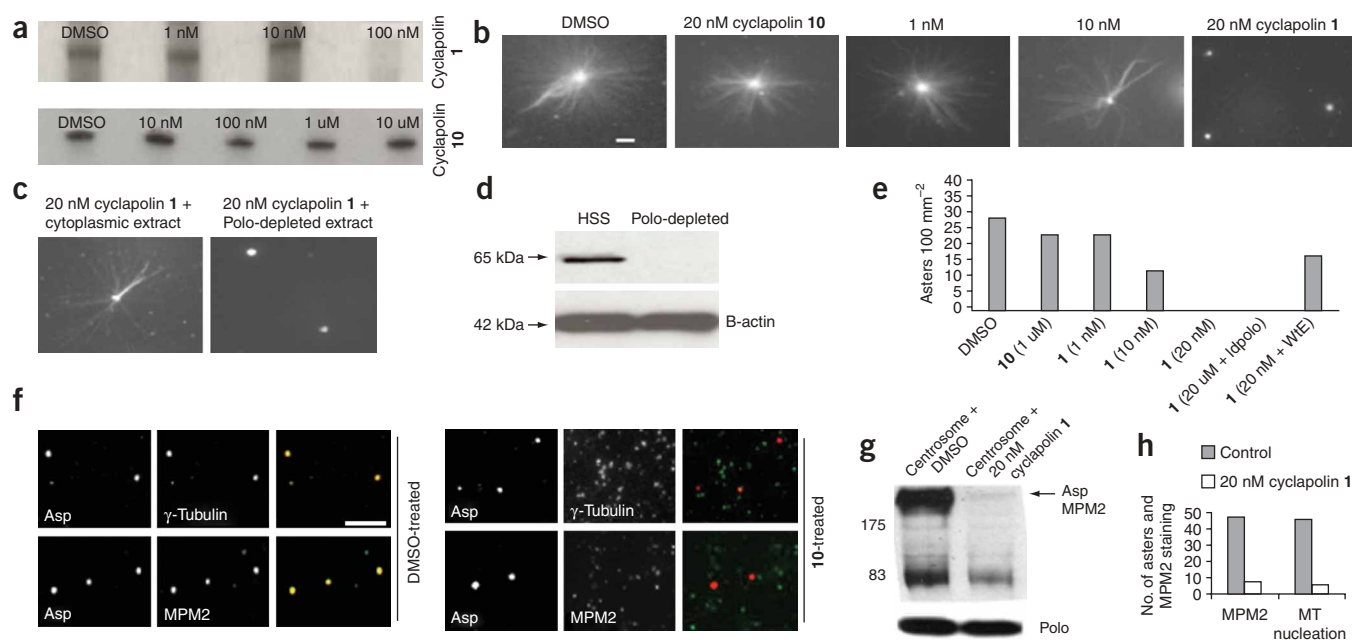


Figure 5 Cyclapolin 1 inhibits the nucleation of microtubules by centrosomes *in vitro*. (a) Inhibition of the phosphorylation of casein by *D. melanogaster* Polo kinase by **1** but not **10**. **1** is an effective inhibitor between 10 and 100 nM. Phosphorylated casein is shown after SDS-PAGE and autoradiography. (b) Inhibition of microtubule nucleating properties of centrosomes by **1**. Centrosomes are pelleted onto a coverslip to which rhodamine-labeled tubulin is then added. Numbers of microtubules nucleated are reduced by 10 nM **1**, and nucleation is absent at 20 nM. Scale bar represents 2 μ m. (c, d) Untreated high-speed cytoplasmic supernatant (HSS) rescues the nucleating ability of centrosomes treated with 20 nM **1**. This rescuing ability is lost after immunodepletion of Polo kinase. The effective depletion of Polo is illustrated in the western blot showing two aliquots of nondepleted and one aliquot of Polo-immunodepleted (Idpolo) cytoplasm. (e) Histogram quantitating the outcome of experiments illustrated in b and c. WtE, wild-type extract. (f) Immunostained centrosomes after **1** treatment showing loss of γ -tubulin and MPM2 reactivity. Monochrome panels are labeled with the identity of the protein detected; merged images are shown in the right-hand panel. Scale bar represents 10 μ m. (g) Western-blot analysis of partially purified centrosomes that have been treated with 20 nM **1** to reveal Polo kinase and proteins with MPM2 epitopes. Lane 1, partially purified centrosomes treated with 0.1% DMSO; lane 2, partially purified centrosomes treated with 20 nM **1**. Polo kinase is not lost from centrosomes although MPM2 reactivity is lost after **1** treatment. (h) Quantitation of the experiment shown in f. MT, microtubule.

microtubules that are not nucleated in the absence of centrosomes (Supplementary Fig. 3). When **1**-treated extract was added to salt-stripped centrosomes, it failed to restore MPM2 staining and recruitment of γ -tubulin, and the ability of the centrosomes to nucleate asters of microtubules was not rescued (Fig. 6c). These properties could be restored if the coverslip was then bathed in untreated high-speed cytoplasmic supernatant (Fig. 6d). Thus chemical inhibition of cytoplasmic Polo kinase prevents both recruitment of the γ -TuRC and generation of MPM2 epitopes on the core centrosome.

DISCUSSION

Generation of a hypothetical structure for Plk1 through homology modeling and subsequent *in silico* molecular docking of known ligands led us to the discovery that benzothiazole *N*-oxide derivatives are inhibitors of Plks. We therefore demonstrate that a structure-guided approach is a valid strategy for the identification of new chemical starting points for Plk inhibition that should be generally applicable to new pharmacophore discovery for this kinase. Members of the benzothiazole chemical series, the cyclapolins, show high selectivity for Plks over many other kinases. This is indicated not only by the selective inhibition of protein kinase activity *in vitro* but also by the cellular phenotypes obtained both in *D. melanogaster* and in HeLa cells, and by the effects upon the nucleation of microtubules by isolated centrosomes.

Treatment of either *D. melanogaster* S2 cells or human HeLa cells with **1** leads to an elevated frequency of mitotic cells. A common

outcome in both cell types is the shortening of the mitotic spindle. Time-lapse studies in the *D. melanogaster* cells indicated that spindles can initially collapse to give transient monopolar structures from which bipolarity is reestablished, apparently as a result of the nucleation of microtubules by chromosomes. Such spindle collapse followed by the regeneration of a bipolar structure with centrosomes at only one pole has been previously described to occur after the depletion of either microtubule stabilizing (for example, Orbit and Mast) or destabilizing (for example, Klp10A or Klp67A) proteins from *D. melanogaster* S2 cells^{36,37}. Spindle collapse with subsequent resumption of some degree of bipolarity is also seen in *D. melanogaster* spermatocytes in mutants that lack components of the γ -TuRC^{38,39}. Thus Polo may have a role in promoting the activity of one or more proteins that regulate addition or removal of tubulin subunits to microtubules, in addition to its known effect of regulating concentrations of the γ -TuRC at the centrosome.

In neither HeLa cells nor S2 cells do the phenotypes resulting from the chemical inhibition of Plk1 or Polo, respectively, correspond precisely to those resulting from their downregulation by RNAi. In HeLa cells, Plk1 RNAi leads to the formation of either monopolar spindles or bipolar spindles with one or more unfocused poles³² (our data, Supplementary Fig. 1), whereas **1** results in shortened spindles. Depletion of *D. melanogaster* Polo kinase in P-element insertion mutants or by RNAi leads to metaphase arrest with bipolar spindles that lack the γ -TuRC at centrosomes^{33,34}. In contrast, chemical inhibition of Polo while mitosis was in progress did not lead to any

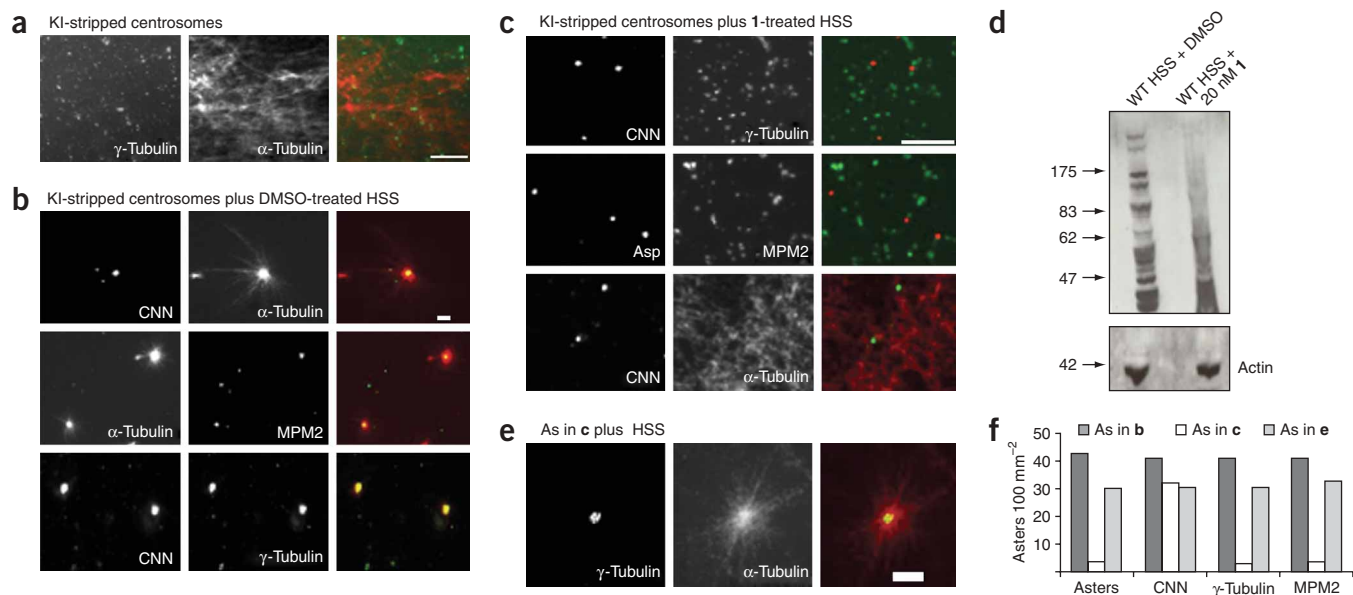


Figure 6 Effects of cyclapolin 1 on the restoration of the microtubule nucleating activity of salt-stripped centrosomes by cytoplasmic extracts. **(a)** Partially purified centrosome preparation treated with 1 M KI and then incubated with rhodamine-labeled tubulin. Centrosomes lose γ -tubulin and microtubule nucleation activity when treated with 1 M KI. Scale bar represents 10 μm . **(b)** Partially purified centrosomes treated with 1 M KI, incubated with rhodamine-labeled tubulin and high-speed cytoplasmic supernatant (HSS) treated with 0.1% DMSO. The preparation is stained to reveal centrosomin (CNN), γ -tubulin and α -tubulin as indicated. Scale bar represents 2 μm . **(c)** Partially purified centrosomes treated with 1 M KI, incubated with rhodamine-labeled tubulin and HSS treated with 20 nM **1**. The preparation is stained to reveal CNN, γ -tubulin, Asp and the MPM2 epitope. These data show that loss of MPM2 epitope and γ -tubulin recruitment are attributable to Polo inhibition. Scale bar represents 10 μm . **(d)** Western blot of HSS treated with 20 nM **1** reveals loss of the MPM2 epitope from several proteins in the HSS. WT, wild type. **(e)** KI-stripped centrosomes were incubated with HSS treated with 20 nM **1**. Coverslips were then washed and incubated with untreated HSS. Microtubule nucleating ability, γ -tubulin and MPM2 phosphoepitope were restored. Scale bar represents 2 μm . **(f)** Quantitation of experiments in **b–e**.

substantial loss of the γ -TuRC from the centrosome but did lead to formation of monopolar spindles and bipolar spindles in which only one pole was organized. We offer two possible explanations for these differences. First is the possibility that we have not fully inhibited all kinase activity in **1**-treated cells, which is possibly a result of restricted uptake of the compound. This is suggested by the greater sensitivity of centrosomes and loss of γ -tubulin from the spindle poles after **1** treatment *in vitro*. However, the phenotypes of cells treated with **1** are very similar to those we first reported for the original mutant *polo*¹ allele^{1,2}, in which the mutation produces protein with reduced catalytic activity rather than depleting protein concentrations⁴⁰. Although this could indicate partial loss of function, it may also suggest that the different responses to **1** treatment and RNAi are a consequence of chemically inhibiting the catalytic activity rather than depleting the protein. The explanation for this may reflect the requirement for a functional Polo box to target Plk with a kinase-dead mutation to be able to block the function of wild-type enzyme⁴¹. Treatment with a small-molecule inhibitor that interacts with the ATP binding site might therefore result in the accumulation of inactive kinase at multiple sites, which would interfere with the formation of functional complexes at these sites. RNAi on the other hand would downregulate protein concentrations and thereby remove kinase from all of the binding sites. The resulting differences in the molecular architecture of these sites could account for the different consequences of chemical inhibition or inactivating mutations versus loss of protein in protein-null mutants or after RNAi.

Analysis of the effects of **1** upon the *in vitro* nucleation of microtubules by isolated centrosomes indicates that Polo kinase is required not only for establishing microtubule nucleation by this

organelle, but also for maintaining nucleation. Previous studies on the nucleation of microtubules by isolated *D. melanogaster* centrosomes have focused on the ability of a cytoplasmic extract to restore microtubule nucleating activities to salt-stripped centrosomes. In many ways, this models the mitotic maturation of centrosomes originally reported in the late nineteenth century by Boveri and now known to be a result of recruitment of microtubule-nucleating molecules⁴². The critical components of this cytoplasmic extract in *D. melanogaster* are the γ -TuRC and Asp^{43,44}. Polo, stabilized by heat shock protein 90 (Hsp90; ref. 45), is required to phosphorylate and activate Asp³⁵ and to recruit the γ -TuRC to the centrosome^{33,34}. We have consistently demonstrated by inhibiting Polo kinase in an *in vitro* system that **1** prevents recruitment of γ -TuRC from a cytoplasmic extract onto salt-stripped centrosomes. This contributes to a failure to restore microtubule nucleation. The concentrations of **1** required to achieve this are equivalent to those required to inhibit Polo kinase activity in the *in vitro* kinase assay. MPM2 epitopes are also not regenerated on such centrosomes, and the spectrum of proteins showing loss of the MPM2 epitope in the cytoplasmic extract is very similar to that seen in *polo* mutants⁴⁶. We note that Asp has been reported to interact with Klp10A and the dynein–dyactin complex to maintain focused spindle poles⁴⁷. Thus it is possible that Polo kinase phosphorylates several components of this complex to regulate their activity. In any event it will be of considerable future interest to identify the set of Polo substrates that have MPM2 epitopes in this cytoplasmic extract and in association with centrosomes.

Our studies of **1** have now also revealed that mature (non-salt-stripped) centrosomes lose their microtubule nucleating activity after inhibition of Polo kinase by **1**. Notably such centrosomes also lose their

MPM2 epitopes, which suggests that interaction of centrosomally associated Polo kinase with **1** gives the opportunity for counteracting phosphatases to access their substrates. The loss of the ability of such centrosomes to nucleate microtubules could be accounted for by the dephosphorylation of Asp. Indeed, the electrophoretic mobility of one of these proteins that loses MPM2 reactivity suggests that it is Asp. However, the γ -TuRC is also lost from the centrosome after this treatment, which indicates not only that there is a requirement for Polo in γ -TuRC recruitment but also that continued activity or correct conformation of the kinase is needed to maintain the association of the complex with the centrosome. Such loss of the γ -TuRC from the centrosome is expected upon mitotic exit. Thus downregulation or destruction of Plks at this time may be the single primary requirement for the centrosome to shift from the mitotic to the interphase state.

The availability of a selective Polo kinase inhibitor offers the means of analyzing many aspects of the dynamics of the mitotic process. It also opens the door to a greater variety of biochemical experiments targeted to identify substrates of this mitotic regulator using reconstituted systems for analyzing aspects of mitotic progression. The studies with **1** suggest the existence of a cellular phenotype distinct from that observed with siRNA knockdown of Plk1 protein concentrations, and therefore they have significant implications for anticancer therapy. These results as a whole indicate that development of chemical inhibitors of Polo kinase offers a promising route toward the treatment of human cancer.

METHODS

Plk1 expression and purification. The Plk1 open reading frame (X75932) was amplified from a fetal lung complementary DNA library (Clontech) using primers incorporating restriction enzyme sites. The 5' primer (5'-GCCGCTAGCGACGATGACGATAAGATGAGTGCTGCAGTGACTGCAGGGAAGC-3') had an *NheI* site upstream of the ATG start codon. The 3' primer (5'-GGAATCTT AGGAGGCTTGAGACGG-3') incorporated an *EcoRI* site downstream of the stop codon. The PCR product was subcloned into the *NheI/EcoRI* sites of a baculovirus expression vector (pSSP1) derived from pFastBac Hta (Invitrogen). Cloning into this vector resulted in a hexahistidine-tag fusion at the N terminus of the Plk1 construct. Sf9 strain cells of a passage number less than 20 were split back to give a 300-ml culture volume, at a cell density of 1.5×10^6 cells ml⁻¹. Cells were only used for expression in logarithmic growth phase. Plk1 baculovirus (from P2 amplification) was added to give a multiplicity of infection of 3; this is equivalent to three virus particles for each insect cell. The flasks were incubated at 27 °C, with shaking at 100 r.p.m., for 48 h. On harvest, cell density and viability were determined, and the cultures were spun down at 2,500 r.p.m. for 5 min and washed with ice-cold (0 °C) phosphate-buffered saline. The wash was re-spun at the same speed and the pellet was snap frozen.

Plk1 protein was purified on a metal affinity column. The insect cell pellet was lysed in a buffer (10 mM Tris-HCl, pH 8.0, 150 mM NaCl, 5 mM β -mercaptoethanol, 1 mM PMSF, 1 mM benzamidine, 20 mM imidazole and protease inhibitor cocktail (Sigma)) and the precleared supernatant was loaded onto Ni-NTA-agarose (Qiagen). The affinity column was washed with the lysis buffer and the bound protein was eluted with 250 mM imidazole in the same buffer. After overnight dialysis against 25 mM Tris-HCl, pH 7.5, 100 mM NaCl, 1 mM DTT, 1 mM PMSF, 1 mM benzamidine, protease inhibitor cocktail (Sigma) and 10% glycerol, the purified protein was stored at -70 °C until used.

Construction, expression and purification of Cdc25C. Using standard techniques a full-length Cdc25C clone was isolated by PCR from HeLa mRNA and inserted on a *BamHI-HindIII* fragment into the plasmid pRsetA. The N-terminal Cdc25C fragment (encoding residues 1–300) was excised from this vector and inserted into the plasmid pET28a (between the *NcoI* and *BamHI* sites). Expression was under the control of the T7 promoter, and the encoded protein contains a hexahistidine tag at the C terminus. The vector was transformed into *E. coli* strain BRL(DE3) pLysS for expression experiments. The protein was expressed in BL21(DE3) RIL bacteria cells that were grown in

LB medium at 37 °C until optical density at 600 nm of 0.6 was reached. Expression was induced with 1 mM IPTG, and the bacterial culture was grown further for 3 h. The bacteria were harvested by centrifugation and the cell pellet resuspended in 50 mM Tris, pH 7.5, and 10% sucrose, flash frozen, and stored at -70 °C until used. Purification of the protein was then carried out by lysing the bacterial pellet in 10 ml of lysis buffer (10 mM Tris-HCl, pH 8.0, 150 mM NaCl, 5 mM β -mercaptoethanol and 20mM imidazole) supplemented with a cocktail of protease inhibitors and sonicated six times at 20-s bursts. The lysate was then centrifuged for 15 min at 15,000 r.p.m. and filtered through a 0.45-mm filter. The sample was then loaded onto a Ni-NTA agarose column and washed several times, and then the Cdc25 protein was eluted with a buffer containing 10 mM Tris-HCl, pH 8.0, 100 mM NaCl, 5 mM β -mercaptoethanol, 0.02% Nonidet P-40 (Calbiochem) and 250 mM imidazole. The eluate was then dialyzed, concentrated, snap frozen in liquid nitrogen and stored at -70 °C until used.

D. melanogaster kinase assay. *D. melanogaster* Polo kinase assays were performed as previously described⁴⁰, using baculovirus-expressed Polo kinase. Enzyme was immunoprecipitated using antibody to mouse Polo (M294) and protein A beads that were incubated with increasing concentrations of **1** or **10** for 20 min. 5 μ l of 1 μ g ml⁻¹ of dephosphorylated casein was added to an equal volume of 2 \times kinase buffer (20 mM HEPES, pH 7.5, 150 mM KCl, 10 mM MgCl₂, 2 mM DTT and 1 mM EGTA). To this mixture was added 5 μ l of protein A beads with immunoprecipitated Polo and 1 μ l [γ -³²P]ATP (10 mCi ml⁻¹, Amersham), and 1.0 μ l of 2 mM ATP. The mixture was incubated at 20 °C for 20 min. The phosphorylated substrates were identified by autoradiography after SDS-PAGE.

Molecular modeling. The homology model for Plk1 was generated using the program module Homology within the molecular-modeling package InsightII (Accelrys), using PKA as a template structure. The sequence containing the kinase domain of PLK1 (residues 1–356) was used in a FASTA sequence and structural search in order to find the closest sequence-related kinases for which experimental structural information is available. The closest match of known structure is that of the cyclic AMP-dependent protein kinase PKA, which has a sequence identity of 31% and similarity of 51% in relation to PLK1. Sequence alignment of the PLK1 kinase domain with PKA, and with CDK2 and the mitogen-activated protein kinase ERK2, which were also among the most homologous structures, indicated that the minimal kinase domain included residues 52–308. Using a combination of the three structures to generate coordinates for the regions that had the highest identity in each kinase, a model structure for the kinase domain was constructed. The strategy involved using PKA to define the structurally conserved regions from which the coordinates were subsequently transferred. The final model structure was then checked against databases of protein structures for bond-length and dihedral-angle violations. The results indicated that these as a whole were within acceptable limits, with >80% of residues having backbone dihedral-angle combinations within the allowed region in Ramachandran space.

Compounds were docked with the Plk1 homology model using the Affinity program within InsightII and implementing a molecular-dynamics docking routine. The binding site was defined as an 8-Å radius from the center of a ligand placed in the ATP site. The calculation was performed using the consistent valence force field (CVFF) in a two-step process and an implicitly derived solvation model and geometric hydrogen-bond restraints. Initially, the inhibitor was minimized into the ATP cleft, using a simple nonbonded method in which the coulombic and Van der Waals terms are scaled to 0 and 0.1, respectively. The refinement phase involved molecular dynamics calculated over 5 ps in 100-fs stages; the temperature was scaled from 500 K to 300 K, followed by a final minimization over 1,000 steps using the Polak-Ribiere conjugate gradient method. The docked structures were ranked energetically using the in-house-developed programs Calsor and Calsorcont and the Ludi module of InsightII.

Centrosome purification and microtubule nucleating assays. Purification of centrosomes from *D. melanogaster* embryos, immunofluorescence and complementation assays on KI-treated centrosomes were carried out as previously described^{43,44,48}. **1** or **10** was incubated either with centrosome fractions or

with high-speed embryonic extract for 20 min at room temperature (25 °C) before the microtubule nucleating assays were performed.

Immunodepletion and western blots. Polo kinase was immunodepleted from 100 µl of *D. melanogaster* high-speed embryonic extract using the antibody to Polo (MA294) (20 to 50 µg)⁴⁴. High-speed embryonic extracts were incubated with **I** at room temperature for 20 min and subjected to SDS-PAGE, and the proteins were transferred to nitrocellulose membrane by electroblotting. The membranes were processed as previously described⁴⁰.

Immunofluorescence analysis. S2 and HeLa cells were incubated with **I** for 24 h before fixation and stained⁴⁹ before observation using an Axiovert 200M microscope (Carl Zeiss MicroImaging, Inc.). The following antibodies were used: rat anti- α -tubulin-YL1/2 (Oxford Biosciences; 1:50) and mouse anti- γ -tubulin-GTU88 (Sigma; 1:100).

Live cell imaging and analysis. For time-lapse microscopy, an S2 line expressing GFP-tubulin was grown on clean no. 1 1/2 thickness coverslips. Once a diving cell was seen, **I** was added. Time-lapse microscopy was performed on an Axiovert 200 microscope fitted with a Perkin Elmer Spinning Nipkow disk confocal head. Cells were maintained at 25 ± 1 °C during filming.

Note: Supplementary information is available on the Nature Chemical Biology website.

ACKNOWLEDGMENTS

We would like to thank many colleagues at Cyclacel and the Cancer Research UK Cell Cycle Genetics Group who have contributed to this project. D.M.G. also acknowledges Cancer Research UK Programme support, a Special Cambridge Nehru Bursary and a Cancer Research UK PhD studentship to A.M. We thank M. Savoian and V. Archambault for their comments on the manuscript.

AUTHOR CONTRIBUTIONS

A.M. carried out all the studies involving *D. melanogaster* S2 cells, human cells, and isolated preparations of centrosomes. C.Mc. completed the computational experiments and contributed to project management and manuscript writing. M.M. was responsible for *in vitro* screening and contributed intellectually. C.Me. was responsible for the synthesis of benzothiazole analogs described. C.Mi. and F.S. evaluated effects of **I** on human cell lines. L.C. carried out RNAi and immunostaining of HeLa cells. P.T. and M.W. were responsible for the development and application of LIDAEUS, and P.M.F. contributed to the medical chemistry and project directions.

COMPETING INTERESTS STATEMENT

The authors declare that they have no competing financial interests.

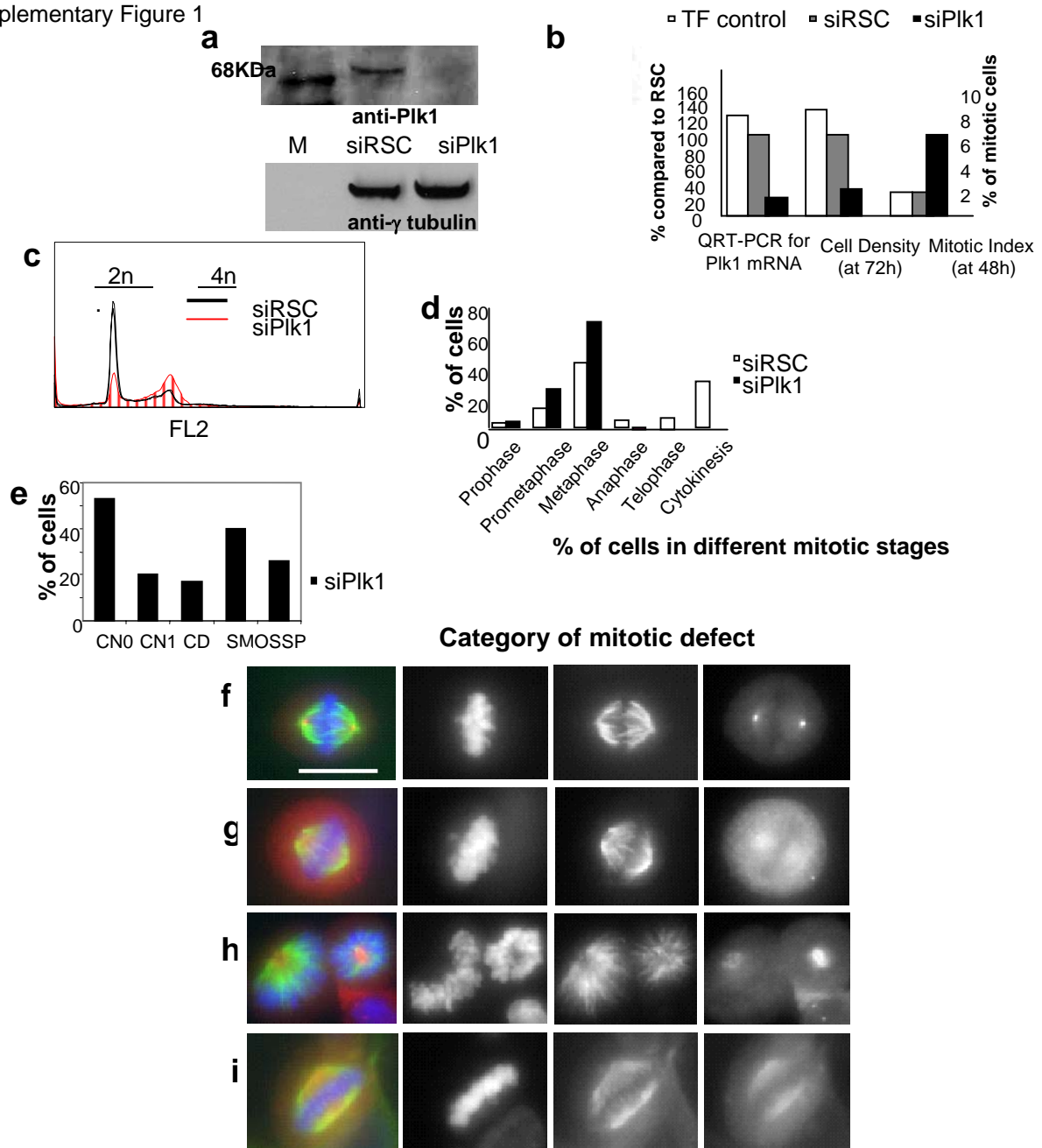
Published online at <http://www.nature.com/naturechemicalbiology>

Reprints and permissions information is available online at <http://npg.nature.com/reprintsandpermissions/>

- Sunkel, C.E. & Glover, D.M. Polo, a mitotic mutant of *Drosophila* displaying abnormal spindle poles. *J. Cell Sci.* **89**, 25–38 (1988).
- Llamazares, S. *et al.* Polo encodes a protein kinase homolog required for mitosis in *Drosophila*. *Genes Dev.* **5**, 2153–2165 (1991).
- McInnes, C., Mezna, M. & Fischer, P.M. Progress in the discovery of polo-like kinase inhibitors. *Curr. Top. Med. Chem.* **5**, 181–197 (2005).
- Glover, D.M., Hagan, I.M. & Tavares, A.A. Polo-like kinases: a team that plays throughout mitosis. *Genes Dev.* **12**, 3777–3787 (1998).
- Elia, A.E., Cantley, L.C. & Yaffe, M.B. Proteomic screen finds pSer/pThr-binding domain localizing Plk1 to mitotic substrates. *Science* **299**, 1228–1231 (2003).
- Leung, G.C. *et al.* The Sak polo-box comprises a structural domain sufficient for mitotic subcellular localization. *Nat. Struct. Biol.* **9**, 719–724 (2002).
- Elia, A.E. *et al.* The molecular basis for phosphodependent substrate targeting and regulation of Plks by the Polo-box domain. *Cell* **115**, 83–95 (2003).
- Jang, Y.J. *et al.* Polo-box motif targets a centrosome regulator, RanGTPase. *Biochem. Biophys. Res. Commun.* **325**, 257–264 (2004).
- Kumagai, A. & Dunphy, W.G. Purification and molecular cloning of Plx1, a Cdc25-regulatory kinase from *Xenopus* egg extracts. *Science* **273**, 1377–1380 (1996).
- Watanabe, N. *et al.* Cyclin-dependent kinase (CDK) phosphorylation destabilizes somatic Wee1 via multiple pathways. *Proc. Natl. Acad. Sci. USA* **102**, 11663–11668 (2005).
- van Vugt, M.A. & Medema, R.H. Getting in and out of mitosis with Polo-like kinase-1. *Oncogene* **24**, 2844–2859 (2005).
- Glover, D.M. Polo kinase and progression through M phase in *Drosophila*: a perspective from the spindle poles. *Oncogene* **24**, 230–237 (2005).
- Hansen, D.V., Loktev, A.V., Ban, K.H. & Jackson, P.K. Plk1 regulates activation of the anaphase promoting complex by phosphorylating and triggering SCFbetaTrCP-dependent destruction of the APC Inhibitor Emi1. *Mol. Biol. Cell* **15**, 5623–5634 (2004).
- Moshe, Y., Boulaire, J., Pagano, M. & Hershko, A. Role of Polo-like kinase in the degradation of early mitotic inhibitor 1, a regulator of the anaphase promoting complex/cyclosome. *Proc. Natl. Acad. Sci. USA* **101**, 7937–7942 (2004).
- Rauh, N.R., Schmidt, A., Bormann, J., Nigg, E.A. & Mayer, T.U. Calcium triggers exit from meiosis II by targeting the APC/C inhibitor XErp1 for degradation. *Nature* **437**, 1048–1052 (2005).
- Liu, J. & Maller, J.L. Calcium elevation at fertilization coordinates phosphorylation of XErp1/Emi2 by Plx1 and CaMK II to release metaphase arrest by cytoskeletal factor. *Curr. Biol.* **15**, 1458–1468 (2005).
- Tung, J.J. *et al.* A role for the anaphase-promoting complex inhibitor Emi2/XErp1, a homolog of early mitotic inhibitor1, in cytoskeletal factor arrest of *Xenopus* eggs. *Proc. Natl. Acad. Sci. USA* **102**, 4318–4323 (2005).
- Hauf, S. *et al.* Dissociation of cohesin from chromosome arms and loss of arm cohesion during early mitosis depends on phosphorylation of SA2. *PLoS Biol.* **3**, e69 (2005).
- Clarke, A.S., Tang, T.T., Ooi, D.L. & Orr-Weaver, T.L. POLO kinase regulates the *Drosophila* centromere cohesion protein MEI-S332. *Dev. Cell* **8**, 53–64 (2005).
- Hornig, N.C. & Uhlmann, F. Preferential cleavage of chromatin-bound cohesin after targeted phosphorylation by Polo-like kinase. *EMBO J.* **23**, 3144–3153 (2004).
- Wong, O.K. & Fang, G. Plx1 is the 3F3/2 kinase responsible for targeting spindle checkpoint proteins to kinetochores. *J. Cell Biol.* **170**, 709–719 (2005).
- Ahonen, L.J. *et al.* Polo-like kinase 1 creates the tension-sensing 3F3/2 phosphopeptide and modulates the association of spindle-checkpoint proteins at kinetochores. *Curr. Biol.* **15**, 1078–1089 (2005).
- Carmena, M. *et al.* *Drosophila* polo kinase is required for cytokinesis. *J. Cell Biol.* **143**, 659–671 (1998).
- Lee, K.S., Yuan, Y.L., Kuriyama, R. & Erikson, R.L. Plk is an M-phase-specific protein kinase and interacts with a kinesin-like protein, CHO1/MKLP-1. *Mol. Cell. Biol.* **15**, 7143–7151 (1995).
- Neef, R. *et al.* Phosphorylation of mitotic kinesin-like protein 2 by polo-like kinase 1 is required for cytokinesis. *J. Cell Biol.* **162**, 863–875 (2003).
- Liu, X., Zhou, T., Kuriyama, R. & Erikson, R.L. Molecular interactions of Polo-like kinase 1 with the mitotic kinesin-like protein CHO1/MKLP-1. *J. Cell Sci.* **117**, 3233–3246 (2004).
- Lindon, C. & Pines, J. Ordered proteolysis in anaphase inactivates Plk1 to contribute to proper mitotic exit in human cells. *J. Cell Biol.* **164**, 233–241 (2004).
- Spankuch-Schmitt, B., Bereiter-Hahn, J., Kaufmann, M. & Strebhardt, K. Effect of RNA silencing of polo-like kinase-1 (PLK1) on apoptosis and spindle formation in human cancer cells. *J. Natl. Cancer Inst.* **94**, 1863–1877 (2002).
- Elez, R. *et al.* Tumor regression by combination antisense therapy against Plk1 and Bcl-2. *Oncogene* **22**, 69–80 (2003).
- Wu, S.Y. *et al.* Discovery of a novel family of CDK inhibitors with the program LIDAEUS: structural basis for ligand-induced disordering of the activation loop. *Structure* **11**, 399–410 (2003).
- Lane, H.A. & Nigg, E.A. Antibody microinjection reveals an essential role for human polo-like kinase 1 (Plk1) in the functional maturation of mitotic centrosomes. *J. Cell Biol.* **135**, 1701–1713 (1996).
- Sumara, I. *et al.* Roles of polo-like kinase 1 in the assembly of functional mitotic spindles. *Curr. Biol.* **14**, 1712–1722 (2004).
- Bettencourt-Dias, M. *et al.* Genome-wide survey of protein kinases required for cell cycle progression. *Nature* **432**, 980–987 (2004).
- Donaldson, M.M., Tavares, A., Ohkura, H., Deak, P. & Glover, D.M. Metaphase arrest with centromere separation in *polo* mutants of *Drosophila*. *J. Cell Biol.* **153**, 663–675 (2001).
- do Carmo Avides, M., Tavares, A. & Glover, D.M. Polo kinase and Asp are needed to promote the mitotic organizing activity of centrosomes. *Nat. Cell Biol.* **3**, 421–424 (2001).
- Goshima, G. & Vale, R.D. The roles of microtubule-based motor proteins in mitosis: comprehensive RNAi analysis in the *Drosophila* S2 cell line. *J. Cell Biol.* **162**, 1003–1016 (2003).
- Laycock, J.E., Savoian, M.S. & Glover, D.M. Antagonistic activities of Klp10A and Orbit regulate spindle length, bipolarity and function *in vivo*. *J. Cell Sci.* **119**, 2354–2361 (2006).
- Sampaio, P., Rebollo, E., Varmark, H., Sunkel, C.E. & Gonzalez, C. Organized microtubule arrays in gamma-tubulin-depleted *Drosophila* spermatocytes. *Curr. Biol.* **11**, 1788–1793 (2001).
- Barbosa, V., Gatt, M., Rebollo, E., Gonzalez, C. & Glover, D.M. *Drosophila* dd4 mutants reveal that gammaTuRC is required to maintain juxtaposed half spindles in spermatocytes. *J. Cell Sci.* **116**, 929–941 (2003).
- Tavares, A.A., Glover, D.M. & Sunkel, C.E. The conserved mitotic kinase polo is regulated by phosphorylation and has preferred microtubule-associated substrates in *Drosophila* embryo extracts. *EMBO J.* **15**, 4873–4883 (1996).
- Liu, X., Zhou, T., Kuriyama, R. & Erikson, R.L. Molecular interactions of Polo-like kinase 1 with the mitotic kinesin-like protein CHO1/MKLP-1. *J. Cell Sci.* **117**, 3233–3246 (2004).

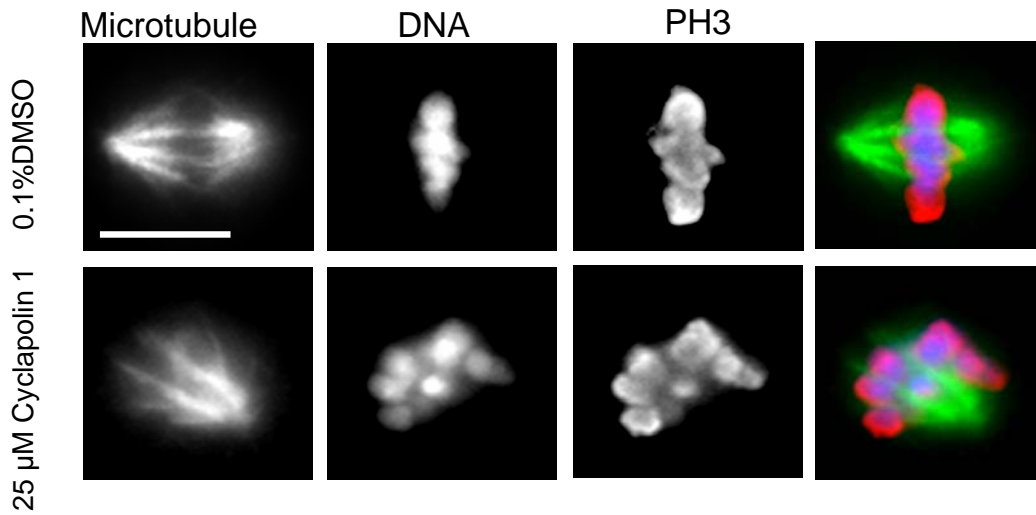


42. Blagden, S.P. & Glover, D.M. Polar expeditions—provisioning the centrosome for mitosis. *Nat. Cell Biol.* **5**, 505–511 (2003).
43. Moritz, M., Zheng, Y., Alberts, B.M. & Oegema, K. Recruitment of the gamma-tubulin ring complex to *Drosophila* salt-stripped centrosome scaffolds. *J. Cell Biol.* **142**, 775–786 (1998).
44. do Carmo Avides, M. & Glover, D.M. Abnormal spindle protein, Asp, and the integrity of mitotic centrosomal microtubule organizing centers. *Science* **283**, 1733–1735 (1999).
45. de Carcer, G., do Carmo Avides, M., Lallena, M.J., Glover, D.M. & Gonzalez, C. Requirement of Hsp90 for centrosomal function reflects its regulation of Polo kinase stability. *EMBO J.* **20**, 2878–2884 (2001).
46. Logarinho, E. & Sunkel, C.E. The *Drosophila* POLO kinase localises to multiple compartments of the mitotic apparatus and is required for the phosphorylation of MPM2 reactive epitopes. *J. Cell Sci.* **111**, 2897–2909 (1998).
47. Morales-Mulia, S. & Scholey, J.M. Spindle pole organization in *Drosophila* S2 cells by dynein, abnormal spindle protein (Asp), and KLP10A. *Mol. Biol. Cell* **16**, 3176–3186 (2005).
48. Moritz, M. & Alberts, B.M. Isolation of centrosomes from *Drosophila* embryos. *Methods Cell Biol.* **61**, 1–12 (1999).
49. Bettencourt-Dias, M. *et al.* SAK/PLK4 is required for centriole duplication and flagella development. *Curr. Biol.* **15**, 2199–2207 (2005).

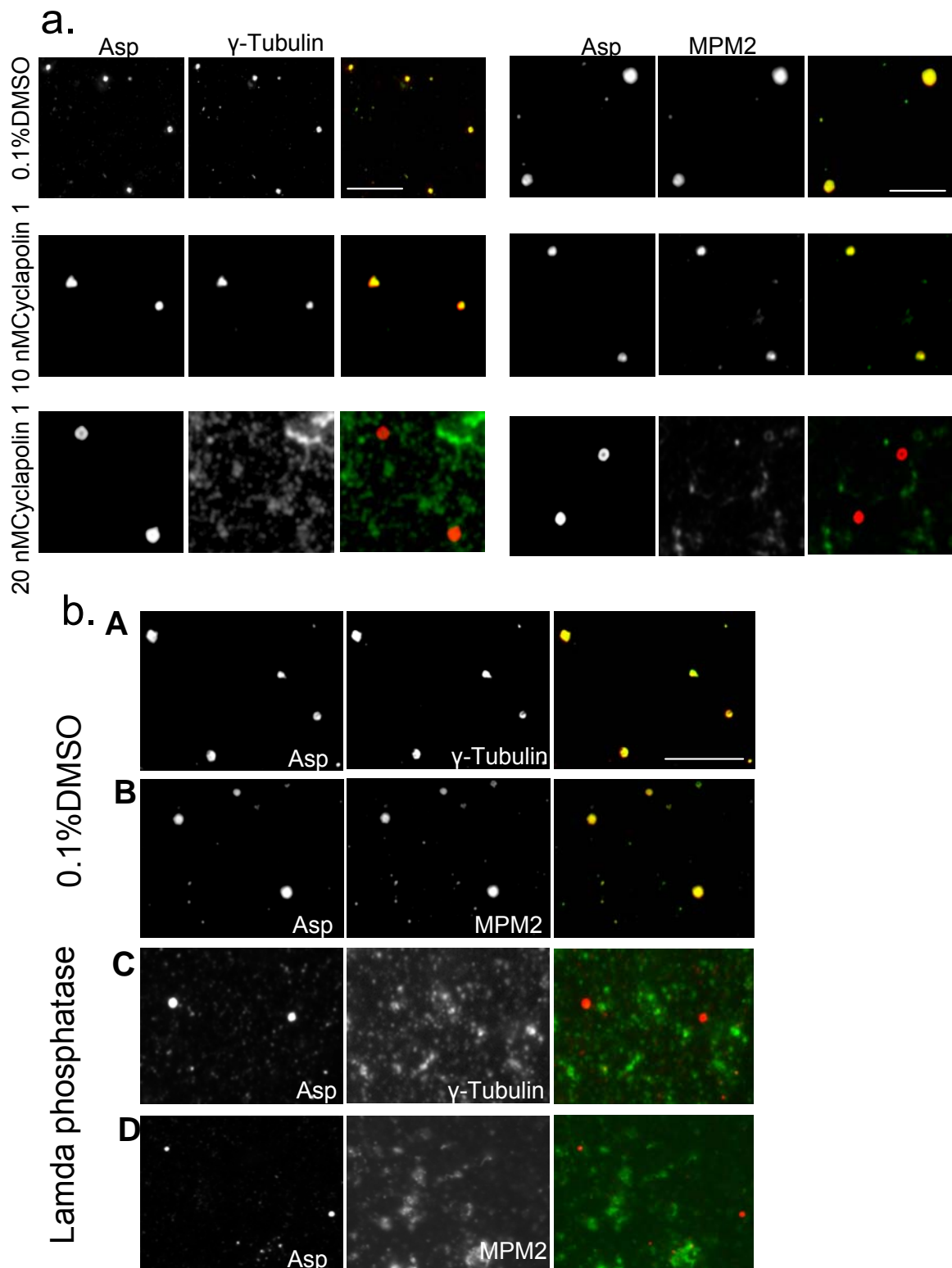


Supplementary Figure 1 Mitotic phenotypes following Plk1 RNAi in HeLa cells

- a** *Immuno-blotting to demonstrates knockdown of Plk1 protein:* HeLa cells were transfected with RSC or Plk1 siRNA (siRSC and siPlk1 respectively) and protein lysates taken at 24h post-transfection. Protein was separated by 12% SDS-PAGE and transferred to nitrocellulose for blotting using anti-Plk1 (Santa Cruz) or anti g-tubulin (Sigma) antibodies. SiRNA towards Plk1 demonstrates significant reduction in protein levels when compared to the RSC control.
- b** *Quantitative assessment of phenotypic parameters:* Assessment of Plk1 mRNA levels by QRT-PCR after siRNA towards Plk1 (siPlk1), demonstrates almost 80% knockdown when compared to treatment with a random sequence control dsRNA oligonucleotide (siRSC). Transfast only (TF control) represents effects of transfecting the lipid vehicle alone. Assessment of cell density after 72h treatment with siPlk1 demonstrates a significant reduction in cell density assayed by nuclear staining with DAPI and quantitated by automated microscopy. TF and RSC controls show the expected cell density. Assessment of mitotic index at 48h after exposure to siPlk1, monitored by staining with anti-phospho-histone H3 antibody and an Alexa595 conjugated secondary antibody, followed with DAPI staining and automated microscopy. This shows a significant increase in mitotic index when compared to TF and RSC controls.
- c** *Increase in G2/M and subG1 cells following Plk1 siRNA treatment:* HeLa cells were transfected with Transfast and siRNA and harvested after 24h. Cells were pelleted and fixed in 70% ethanol overnight at -20°C , and resuspended in propidium iodide and RNase for 30 mins. Fluorescence activated cell sorting was performed on a Beckton and Dickinson LSR. Fluorescence from the FL2 channel is presented: siPlk1 treated cells (red line); RSC control (black line).
- d** *HeLa cells with Plk1 siRNA show a prometaphase/metaphase delay:* Transfected cells were fixed after 24h with a methanol and formalin mix for 15 min, permeabilised and blocked with 0.1% Triton X100 with 1% BSA in PBS before staining with either anti- α or - γ tubulin (1:200) and appropriate Alexa conjugated secondaries (1:500). Quantitative microscopy reveals a significant shift in number of cells in prometaphase/metaphase following Plk1 RNAi.
- e-i** *Plk1 knockdown induces a range of mitotic defects:* Cells exposed to siPlk1 were fixed and stained as above. Analysis by microscopy reveals a range of defects which included a single centrosomal mass (CN1) or no centrosomal staining (CN0) indicated by anti-g-tubulin staining. Alternately, g-tubulin staining was diffuse and centrosomes had positioning defects (CD). Spindle defects observed by anti- α -tubulin staining included monopolar spindles (SMO) and abnormal or splayed spindle poles (AS/SSP). These defects were essential absent in control cells. Columns represent: merged image (left), DNA (second column), α -tubulin (third column) and g-tubulin (right hand). The first row **f**) represents siRSC treated control cells; **g**) Plk1 RNAi cells with SSP and CNO defects; **h**) Plk1 RNAi cells with SMO and CN1/CD defects, and **i**) Plk1 RNAi cells with CD defects. Scale bar represents 10 μm .



Supplementary Figure 2. Cyclapolin-1 (Compound 1) does not affect phosphorylation of histone H3 on Serine 10 Control (a) or Compound 1 treated cells (b) (see legend to Fig. 4) were stained to reveal DNA (blue), microtubules (green) and phospho-histone H3 (red).



Supplementary Figure 3a. Dose dependent loss of gamma-tubulin and MPM-2 phospho-epitope from Cyclapolin-1 treated centrosomes.

Partially purified centrosomes were treated with 0.1% DMSO carrier alone or with either 10 or 20 nM **1** and stained to reveal gamma-tubulin, the MPM-2 phosphoepitope and the Asp protein as indicated. Loss of gamma-tubulin and MPM-2 occurs at the concentration at which Polo kinase activity is inhibited.

b. Effects of Lambda Phosphatase upon partially purified centrosomes.

Partially purified preparation of centrosomes was treated with either 0.1% DMSO (a, b) or NN units/ml lambda phosphatase (c, d) and stained to reveal the indicated antigens. Lambda phosphatase treatment results in the loss of gamma-tubulin and the MPM2-phospho-epitope but not the abnormal spindle protein, Asp.

Supplementary Table 1. Selectivity of Cyclapolin 9 and 1 respectively

Kinase	Cyclapolin 9	Cyclapolin 1
Plk1	0.5	0.02
Cdk2/E	>100	>100
Cdk2/A	>100	>100
Cdk1/B	>100	>100
Cdk4/D1	>100	>100
Cdk7/H	>100	>100
Cdk9/T	>100	>100
CK II	>100	>100
CamK II	>100	>100
MAPK2/ERK	>100	>100
PKC a	>100	>100
Akt/PKB	>100	>100
Abl	>100	>100
GSK3a	>100	>100
Aurora A	>100	>100
PKA	>100	>100
P70S6K	>100	>100
SAPK2	>100	>100

Further testing of compound 6 on an additional panel of 20 kinases extended the selectivity

Supplementary Table 2. In addition Cyclapolin **9** was screened against 21 kinases from UpstateCell signalling. The percentage inhibition of each enzyme at 100 uM of compound.

Enzyme	Activity (% of control)
c-RAF	108 ± 10
CDK2/E	88 ± 4
Chk1	111 ± 7
Chk2	97 ± 10
CSK	45 ± 2
FGFR3	83 ± 10
IGF-1R	98 ± 6
IKK α	115 ± 14
IR	107±12
JNK2 α 2	106±1
MAPKAP-K2	96 ± 11
MEK1	96 ± 6
MKK6	88 ± 5
MSK1	106 ± 5
PDGFR α	108 ± 8
PKC γ	117 ± 15
PKC β II	82 ± 14
Rsk2	105 ± 5
SAPK2b	94 ± 3
SAPK3	120 ± 6
Yes	108 ± 12

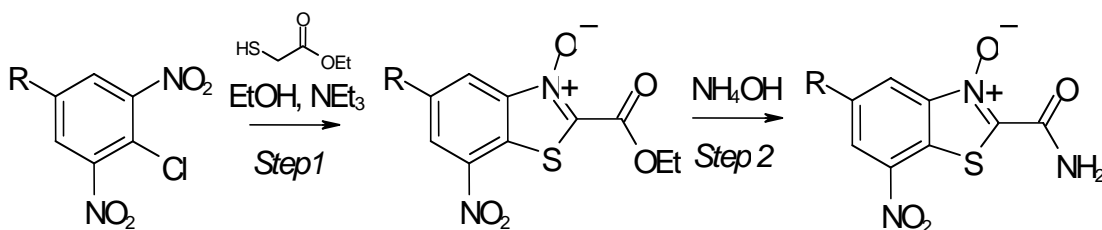
Cytotoxicity of Cyclapolins was tested against three cell lines in a 72 hr MTT assay

Supplementary Table 3

	PIk1 IC50	A549	HeLa	HT29
Cyclapolin 9	0.5	24.8	6.6	7.7
Cyclapolin 1	0.02	14	14	2.8
Cyclapolin 10	>100	72.1	53.6	50.5

Supplementary Methods

Synthesis of benzthiazole N-oxide derivatives



Step 1

Triethylamine (1.1eq) was added to a suspension of 1,3-dinitrobenzyl-2-chloride (1eq) and ethyl thioglycolate (1eq) in ethanol (3cm³) at 10-20°C. Onset of reaction was observed by the solvent beginning to reflux even though the mixture was being cooled in a water bath. On stirring for a further 3h a precipitate formed which was collected by filtration, washed with water followed by methanol and recrystallised from methanol.¹

Step 2

The 2-alkoxycarbonylbenzthiazol-N-oxide 3 (1eq) was suspended in methanol (2cm³) at 20-30°C and the desired amine (1.2eq) added. After stirring for 4h the desired 2-carbamoylbenzthiazol-N-oxide crystallised from solution, was collected by filtration, washed with water followed by methanol and recrystallised from methanol

Cyclapolin-9 (Compound 9)

Compound obtained as a yellow crystalline solid, mp 222-223°C (lit 225-226°C)¹. Anal. RP-HPLC: t_R 13.75 min. (10-70% MeCN). ¹H NMR (DMSO-d₆, 500 MHz): δ_H 8.76 (2H, s, Ar-H and NH), 8.96 (1H, s, Ar-H) and 9.36 (1H, s, NH). ¹³C NMR (DMSO-d₆, 126 MHz): δ_C 122.13, 122.39, 124.31, 127.36, 129.80(q), 143.81, 145.55, 146.73 and 158.28. MS (ESI⁺) m/z 308.01 [M+H]⁺ (C₉H₄N₃O₄F₃S requires 307.21).

Cyclapolin-1 (Compound 1)

Compound obtained as a yellow crystalline solid, mp 255-256°C. C₉H₅N₃O₄F₃S₂ requires M 339.96736, found 339.96739. Anal. RP-HPLC: t_R 15.79 min. (10-70% MeCN). ¹H NMR (DMSO-d₆, 500 MHz): δ_H 8.82 (1H, s), 8.85 (1H, s), 8.90 (1H, s)(2 x Ar-H and NH) and 9.35 (1H, s, NH). ¹³C NMR (DMSO-d₆, 126 MHz): δ_C 125.22, 126.41, 131.86, 132.65, 143.36, 145.28, 146.64 and 158.32; MS (ESI⁺) m/z 339.92 [M+H]⁺ (C₉H₅N₃O₄F₃S₂ requires 339.27).

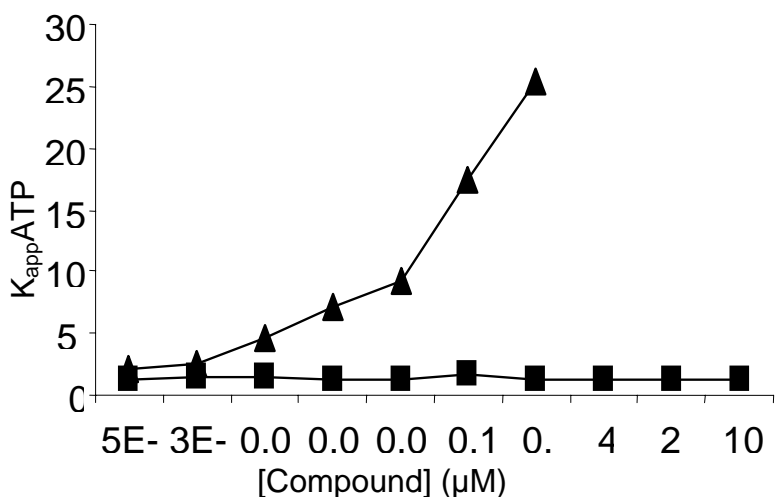
Cyclapolin-10 (Compound 10)

Compound obtained as a yellow crystalline solid, mp 229-230°C (lit 232-233°C)¹. Anal. RP-HPLC: t_R 11.88 min. (10-70% MeCN). ¹H NMR (DMSO-d₆, 500 MHz): δ_H 5.20 (2H, s, NH₂), 8.88 (1H, s, Ar-H), 8.95 (1H, s, Ar-H) and 11.20 (1H, s, NH). ¹³C NMR (DMSO-d₆, 126 MHz): δ_C 122.11, 123.09, 124.31, 127.41, 129.95(q), 143.81, 144.44, 146.25 and 154.35.

Kinase assays

Plk1 kinase activity was assayed using either Casein or the N-terminal domain of the human Cdc25C phosphatase (a natural substrate for Plk1) as substrates. The assays were carried out using a 96-well plate format by incubating Cdc25C (2 $\mu\text{g}/\text{well}$) or Casein (50 $\mu\text{g}/\text{well}$) with varying concentrations of the Ni-NTA purified Plk1 and varying concentrations of the negative, non-transformed host *Sf9* cell lysate in a total volume of 25 μl of 20 mM Tris/HCl buffer pH 7.0, supplemented with 25 mM β -glycerophosphate, 5 mM EGTA, 1 mM DTT and 1 mM NaVO_3 . Reaction was initiated by the addition of 100 μM ATP and 0.5 μCi of $[\gamma\text{-}^{32}\text{P}]\text{-ATP}$. The reaction mixture was incubated at 30°C for 1 h, then stopped with 75 mM aq orthophosphoric acid, transferred onto a 96-well P81 filter plate (Whatman), dried, and the extent of Cdc25C phosphorylation was assessed by scintillation counting using a Packard TopCount plate reader.

Finally a Plot of $K_{\text{app}}\text{ATP}$ for Cyclapolins **9** (\blacktriangle) and **1** (\blacksquare) showed that Plk1 inhibition of the latter compound does not vary with ATP concentration.



Compound Data Index

From the following article

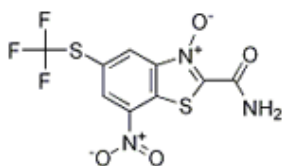
[Inhibitors of Polo-like kinase reveal roles in spindle-pole maintenance](#)

Campbell McInnes, Aveek Mazumdar, Mokdad Mezna, Christopher Meades, Carol Midgley, Fred Scaerou, Lee Carpenter, Mairi Mackenzie, Paul Taylor, Malcolm Walkinshaw, Peter M Fischer & David Glover

Nature Chemical Biology **2**, 608-617 (2006) Published online: 8 October 2006

doi: 10.1038/nchembio825

[BACK TO ARTICLE](#)

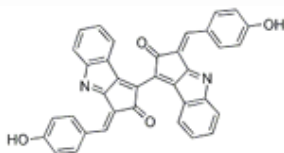


Compound 1

2-Benzothiazolecarboxamide, 7-nitro-5-[(trifluoromethyl)thio]-3-oxide

[View in PubChem : Compound](#)

[View compound page : Compound \(1 KB\)](#) | [Download ChemDraw file of structure : Compound \(3 KB\)](#)

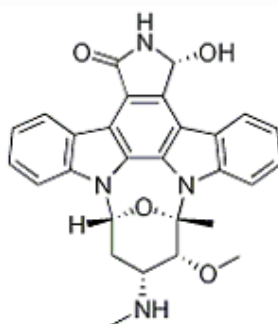


Compound 2

(1,1'-Bicyclopent(b)indole)-2,2'(3H,3'H)-dione, 3,3'-bis((4hydroxyphenyl)methylene)-3,3'-Bis((4-hydroxyphenyl)methylene)-(1,1'-bicyclopent(b)indole)-2,2'(3H,3'H)-dione

[View in PubChem : Compound](#)

[View compound page : Compound \(2 KB\)](#) | [Download ChemDraw file of structure : Compound \(4 KB\)](#)

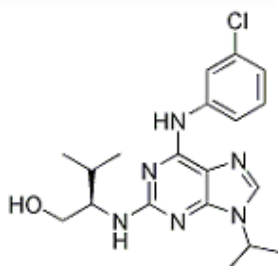


Compound 3

Staurosporine

[View in PubChem : Compound](#)

[View compound page : Compound \(2 KB\)](#) | [Download ChemDraw file of structure : Compound \(4 KB\)](#)

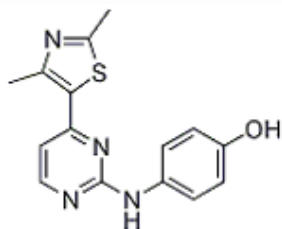


Compound 4

6-((3-chloro)anilino)-2-(isopropyl-2-hydroxyethylamino)-9-isopropylpurine

[View in PubChem : Compound](#)

[View compound page : Compound \(2 KB\)](#) | [Download ChemDraw file of structure : Compound \(3 KB\)](#)

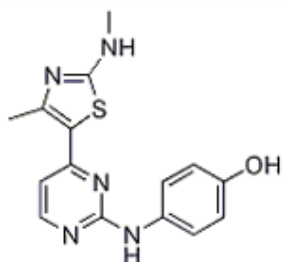


Compound 5

4-[4-(2,4-Dimethyl-thiazol-5-yl)-pyrimidin-2-ylamino]phenol

[View in PubChem : Compound](#)

[View compound page : Compound \(1 KB\)](#) | [Download ChemDraw file of structure : Compound \(3 KB\)](#)

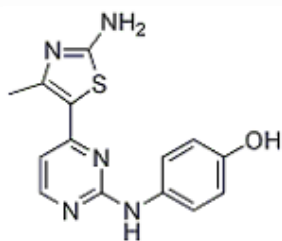


Compound 6

4-[4-(4-Methyl-2-methylaminothiazol-5-yl)pyrimidin-2-ylamino]phenol

[View in PubChem : Compound](#)

[View compound page : Compound \(1 KB\)](#) | [Download ChemDraw file of structure : Compound \(3 KB\)](#)

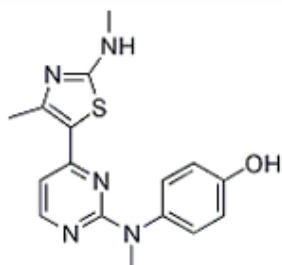


Compound 7

4-[4-(2-Amino-4-methylthiazol-5-yl)pyrimidin-2-ylamino]phenol

[View in PubChem : Compound](#)

[View compound page : Compound \(1 KB\)](#) | [Download ChemDraw file of structure : Compound \(3 KB\)](#)

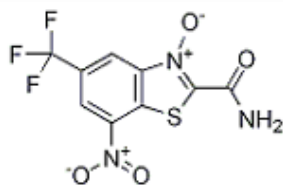


Compound 8

4-[Methyl-4-(4-methyl-2-methylamino-thiazol-5-yl)pyrimidin-2-yl]amino]phenol

[View in PubChem : Compound](#)

[View compound page : Compound \(1 KB\)](#) | [Download ChemDraw file of structure : Compound \(3 KB\)](#)

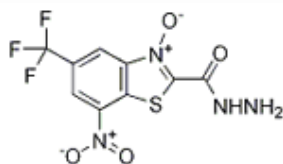


Compound 9

7-Nitro-3-oxy-5-trifluoromethyl-benzothiazole-2-carboxylic acid amide

[View in PubChem : Compound](#)

[View compound page : Compound \(1 KB\)](#) | [Download ChemDraw file of structure : Compound \(3 KB\)](#)



Compound 10

7-Nitro-3-oxy-5-trifluoromethyl-benzothiazole-2-carboxylic acid hydrazide

[View in PubChem : Compound](#)

[View compound page : Compound \(1 KB\)](#) | [Download ChemDraw file of structure : Compound \(3 KB\)](#)